Photoelectron yield spectroscopy and inverse photoemission spectroscopy evaluations of p-type amorphous silicon carbide films prepared using liquid materials

doi: 10.1063/1.4952592

Photoelectron yield spectroscopy and inverse photoemission spectroscopy evaluations of p-type amorphous silicon carbide films prepared using liquid materials

Tatsuya Murakami, Takashi Masuda, Satoshi Inoue, Hiroshi Yano, Noriyuki Iwamuro, and Tatsuya Shimoda

Citation: AIP Advances **6**, 055021 (2016); doi: 10.1063/1.4952592
View online: http://dx.doi.org/10.1063/1.4952592
View Table of Contents: http://scitation.aip.org/content/aip/journal/adva/6/5?ver=pdfcov
Published by the AIP Publishing

Photoelectron yield spectroscopy and inverse photoemission spectroscopy evaluations of p-type amorphous silicon carbide films prepared using liquid materials

Tatsuya Murakami,[1,a] Takashi Masuda,[2,a] Satoshi Inoue,[2] Hiroshi Yano,[3] Noriyuki Iwamuro,[3] and Tatsuya Shimoda[2]
[1]*Center for Nano Materials and Technology, Japan Advanced Institute of Science and Technology (JAIST), 1-1 Asahidai, Nomi, Ishikawa 923-1292, Japan*
[2]*Green Device Research Center, Japan Advanced Institute of Science and Technology, Nomi, Ishikawa 923-1211, Japan*
[3]*Graduate School of Pure and Applied Sciences, University of Tsukuba, Tennoudai, Tsukuba, Ibaraki 305-8573, Japan*

(Received 4 January 2016; accepted 13 May 2016; published online 20 May 2016)

Phosphorus-doped amorphous silicon carbide films were prepared using a polymeric precursor solution. Unlike conventional polymeric precursors, this polymer requires neither catalysts nor oxidation for its synthesis and cross-linkage, providing semiconducting properties in the films. The valence and conduction states of resultant films were determined directly through the combination of inverse photoemission spectroscopy and photoelectron yield spectroscopy. The incorporated carbon widened energy gap and optical gap comparably in the films with lower carbon concentrations. In contrast, a large deviation between the energy gap and the optical gap was observed at higher carbon contents because of exponential widening of the band tail.
[http://dx.doi.org/10.1063/1.4952592]

Amorphous silicon carbide (a-SiC) films have numerous attractive properties such as higher thermal conductivity, better chemical stability, and wider optical gap than those of amorphous silicon (a-Si).[1] Since the early work of Yajima et al.[2] the SiC synthesized by pyrolysis of polycarbosilane has led to numerous publications.[3,4] This polymer-route approach offers potential processing advantage over conventional vacuum-based processes because it is compatible with solution processes, environmental friendly, low-cost, and safe. The technique has been widely used to fabricate SiC fibers with good mechanical properties.[2] However, the SiC has not been applied in semiconducting components because it is difficult to remove the contamination of metal catalyst and oxygen which are required for its synthesis and cross-linkage.[5,6]

In a previous study, we developed polymeric precursor solution (SiC-ink) to prepare semiconducting SiC.[7] An important feature of this polymer is that the synthesis procedure and cross-linkage require neither metal catalyst nor oxidation, resulting in the films with semiconducting properties after sintering. The polymer can be designed to result in a film with Si-rich stoichiometry, whereas the polycarbosilane inevitably provides C-rich stoichiometry. Moreover, the polymer can be doped to form p- or n-type SiC through the dissolution of appropriate compounds.[8] These unusual features satisfy the requirement as a solution-based semiconducting material.

Among the many interesting properties of a-SiC films, a fundamental one is the position of energy levels, i.e., conduction band minima (CBM) and valence band maxima (VBM). The characteristics of these states for conventionally used vacuum-processed a-SiC have been greatly debated theoretically and extensively investigated experimentally.[9,10] However, experimental determinations

[a]Electronic addresses: mtatsuya@jaist.ac.jp and mtakashi@jaist.ac.jp

of the CBM are rare compared to those of the VBM, even in conventionally used a-SiC. The CBM have frequently been estimated on the basis of the VBM and optical-gap E_{opt} according to the approximation CBM = (VBM + E_{opt}). This estimation is plain; however, it underestimates the CBM because the E_{opt} contains exciton binding energies near the band edge.[11]

In the present study, we report our experimental determination of the CBM and VBM of polymer-derived p-type a-SiC films as a function of the films' carbon content. The CBM and VBM were measured continuously by inverse photoemission spectroscopy (IPES) and photoelectron yield spectroscopy (PYS), respectively. This approach eliminates the tail effect based on the exciton binding energies, giving a precise CBM position and energy gap E_g. Identification of the CBM and VBM to obtain a better understanding of the states would open up a frontier of polymer-derived SiC electronics.

The SiC-ink used in these experiments is a low-viscosity, transparent, liquid-state polymer. The ink was synthesized by the hydrosilylation and polymerization of a mixture of cyclopentasilane (CPS)[12] and cyclohexene as sources of Si and C, respectively. Decaborane with a concentration of 3 wt.% was dissolved in the mixture as a dopant. The synthesis procedure has been reported in one of our previous studies.[13] The atomic ratio of C in the ink (C_{ink}) was controlled by varying the cyclohexene/CPS ratio from 0 (C/Si = 0/100) to 0.73 (C/Si = 73/27).

For the deposition of a-SiC films, we developed a thermal chemical vapor deposition method that is conducted under atmospheric pressure using SiC-ink, as shown in Figure 1(a). We refer to this method as liquid-source vapor deposition (LVD).[14,15] As a deposition method in SiC-ink, the advantages of LVD compared to coating methods are its simplicity and low capital outlay in addition to its ability to deposit high-quality films via nonvacuum processes. The SiC-ink (7 μL) was placed in a chamber with a diameter of 80 mm and a depth of 0.5 mm. The chamber was placed directly on a 4-inch substrate, which was subsequently heated on a hot plate at 380°C for 5 min. The evaporated ink filled the chamber as a gas source for SiC and transformed into a-SiC on the substrate via thermal decomposition. Photographic images of the 80 nm films on glass substrates prepared using the SiC-ink with C_{ink} = 0 and 0.73 are shown in Figures 1(b) and 1(c), respectively.

All the procedures were conducted in a nitrogen glove box with an oxygen concentration and a dew point less than 0.5 ppm and 75°C, respectively. Secondary-ion mass spectrometric analysis of boron atoms in the films indicated a boron concentration of 3.3×10^{21} cm^{-3}. Hall measurements conducted in the van der Pauw configuration at room temperature revealed that the main carriers are holes (p-type).

The incorporation of carbon into the films and the formation of Si–C bonds were confirmed by X-ray photoelectron spectroscopy (XPS). Figure 2(a) shows the XPS spectrum for the film prepared using the SiC-ink with C_{ink} = 0.31 as a typical spectrum. The chemical shifts of the peak was corrected using a Si–Si bond energy of 99.5 eV. Regarding Si 2p, the peak splits into two components

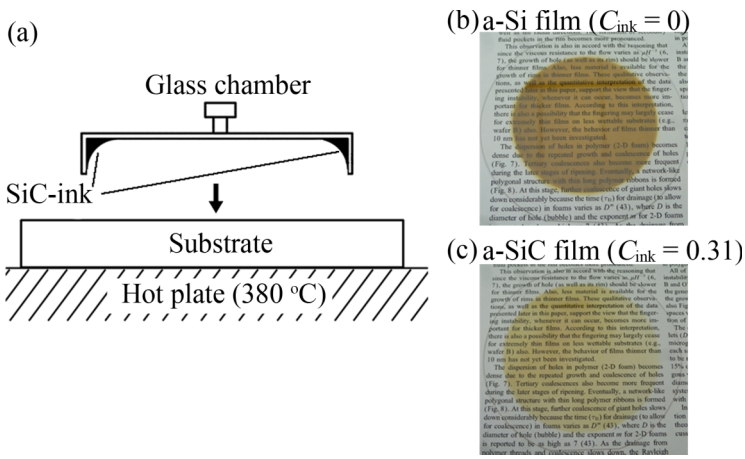

FIG. 1. (a) Schematic of the LVD system. A film with a thickness of 80 nm was obtained when 7 μL of the SiC-ink of was placed in the chamber. (b) The 80-nm-thick films prepared using the SiC-ink with C_{ink} = 0 (i.e., Si-ink) and (c) C_{ink} = 0.31.

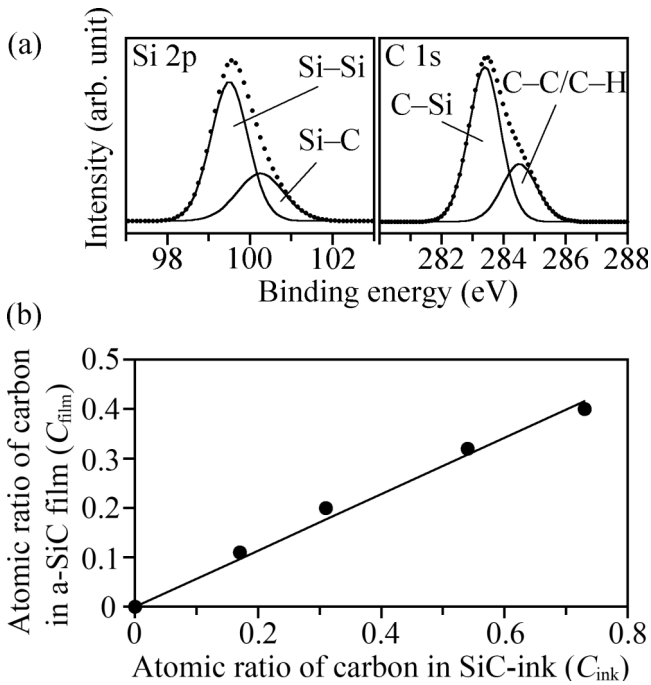

FIG. 2. (a) The Si 2p and C 1s band of a-SiC film prepared using the SiC-ink with $C_{ink} = 0.31$. The closed circles and solid lines represent experimental and fitted data, respectively. Gaussian/Lorentzian function were employed for the fitted lines. (b) Correlation of the Si/C stoichiometry between the SiC-ink and the resultant a-SiC films. The closed circles and solid line represent experimental and fitted data, respectively.

at binding energies of 99.5 and 100.3 eV because of the coexistence of Si–Si and Si–C bonds,[16] respectively, indicating the incorporation of carbon into the silicon network as Si–C bonds. As for C 1s, the peak also splits into two components at binding energies of 283.3 and 284.5 eV, which is attributed to C–Si and C–C/C–H, respectively.[16]

The correlation of the Si/C stoichiometry in the SiC-ink and that in the resultant a-SiC film is presented in Figure 2(b), where the vertical and horizontal axes represent the atomic ratio of C in the film (C_{film}) and C_{ink}, respectively. The C_{film} was evaluated on the basis of the integrated intensity of Si 2p and C 1s bonds measured by XPS, whereas the C_{ink} was calculated from the composition ratio of CPS and cyclohexene. The plot shows a linear relationship with a proportionality factor of 0.57. One distinguishing feature is that the SiC-ink invariably results in Si-rich a-SiC films.

XPS measurements revealed that the incorporated C increased the number of Si–C bonds in the films, as shown in Figure 3(a), where the ratio of Si–C bonds to the total number of Si bonds in the films was estimated from the Si–Si and Si–C bands at 99.5 and 100.3 eV, respectively, for films with various C_{film}. Concomitantly, the incorporated Si–C bonds widened the E_{opt} from 1.56 eV ($C_{film} = 0$; i.e., a-Si) to 2.03 eV ($C_{film} = 0.40$), as shown in Figure 3(b), as a consequence of the replacement of Si–Si bonds by stronger Si–C bonds.[17,18] The E_{opt} was estimated from the equation $(\alpha E)^{0.5} = B^{0.5}(E - E_{opt})$, i.e., a Tauc plot,[19] where α is the optical absorption coefficient obtained from transmittance and reflectance data, B is a constant, and E is the photon energy in eV. The values of E_{opt} were quoted from an our previous study in which Tauc plots were reported.[13] Figure 3(a) and 3(b) indicate that E_{opt} was governed by the quantity of Si–C bonds in the film, which was, in turn, controlled via the cyclohexene-to-CPS ratio in the SiC-ink.

The VBM and CBM for the films with various C_{film} were measured by PYS and IPES, respectively. The Fermi level for all of the films was referenced to that of an Au film. The primary feature of PYS is that the VBM is obtained with higher resolution compared to that obtained by conventional XPS. An applied photon energy ranging from 4.0 to 9.0 eV with a resolution of 0.02 eV was employed for the measurements, where a monochromatic D_2 light source was used.

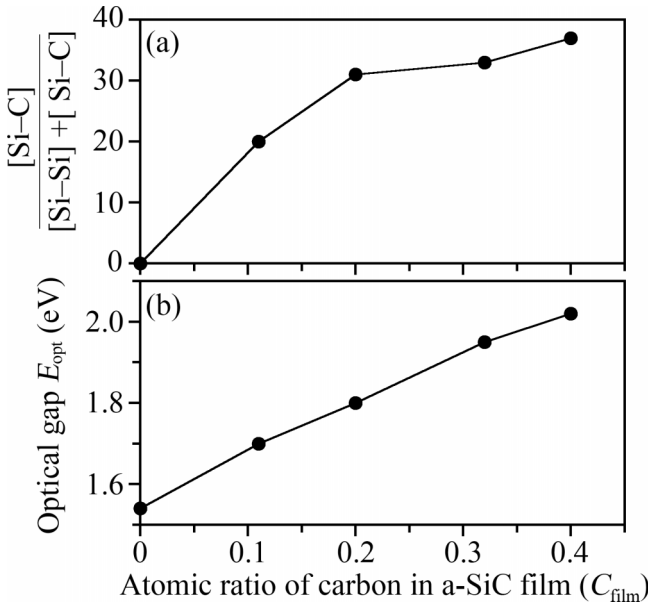

FIG. 3. (a) Ratio of Si–C bonds to the total number of bonded Si in the films as a function of C_{film}. The ratio was estimated from the Si 2p band in the XPS spectra. (b) E_{opt} as a function of C_{film}. The values of E_{opt} were quoted from a reference.[13]

The photoelectron yield was obtained by dividing the photocurrent by the incident photon rate at each photon energy.

Figure 4(a) shows the PYS spectra of films with various C_{film} deposited onto conductive Si substrates. Moreover, the intensity and energy with respect to the vacuum level are plotted on the vertical and horizontal axes, respectively. Linear behavior was observed in the spectra, which means that the spectra can be used to define the VBM by linear extrapolation to zero, as shown schematically by the solid lines and arrows in Figure 4(a). As expected, the incorporation of C caused a shift of the edge toward the lower-energy side as a result of gap widening resulting from the replacement of Si–Si bonds by stronger Si–C bonds.

In the IPES measurements, bremsstrahlung isochromatic spectroscopy mode with a scanning electron energy from 4 to 15 eV with a resolution of 0.6 eV was employed. The electron gun emits monochromatic electrons to a sample, where they couple to unoccupied electron states. Therefore, IPES enables the direct determination of the CBM.[20] The IPES spectra of a series of films with increasing C contents are shown in Figure 4(b), which is depicted in the same format as Figure 4(a). The extrapolation of the IPES leading edge as a function of C_{film} shows that the CBM shifted to the higher-energy side upon the incorporation of C.

In both the PYS and IPES spectra, broadening of the exponential region as a result of a greater degree of topological/compositional disorder[21] is observed with increasing C_{film}. As evident in Figure 3(a), the C incorporated into the films increased the number of Si–C bonds, indicating that the distribution of C atoms in the network is likely compositionally ordered. A picture of the a-SiC structure can be described on the basis of FTIR measurements as a disordered a-Si network in which many hydrogen atoms are incorporated in the form of CH_n moieties.[7,8,13] Therefore, most of the topological/compositional disorder might stem from the variety of hydrogen configurations around C atoms (CH, CH_2, and CH_3). The influence of hydrogen on the electronic structure in conventional a-SiC films is well revealed through XPS and Auger measurements.[21]

The measured VBM, CBM, and E_{opt} values are summarized in Table I. The E_g and CBM values estimated from E_g = (CBM − VBM) and CBM = (VBM + E_{opt}), respectively, are also included for comparison. Both the measured VBM and CBM values shifted by 0.7 eV when the C_{film} was increased from 0 to 0.4, which led to the widening of the E_g from 1.6 to 3.1 eV and of the E_{opt} from 1.54 to 2.02 eV. For the amorphous semiconductor materials, the E_g tends to be greater than the E_{opt} because the former represents the gap state between the mobility edge, whereas the latter represents

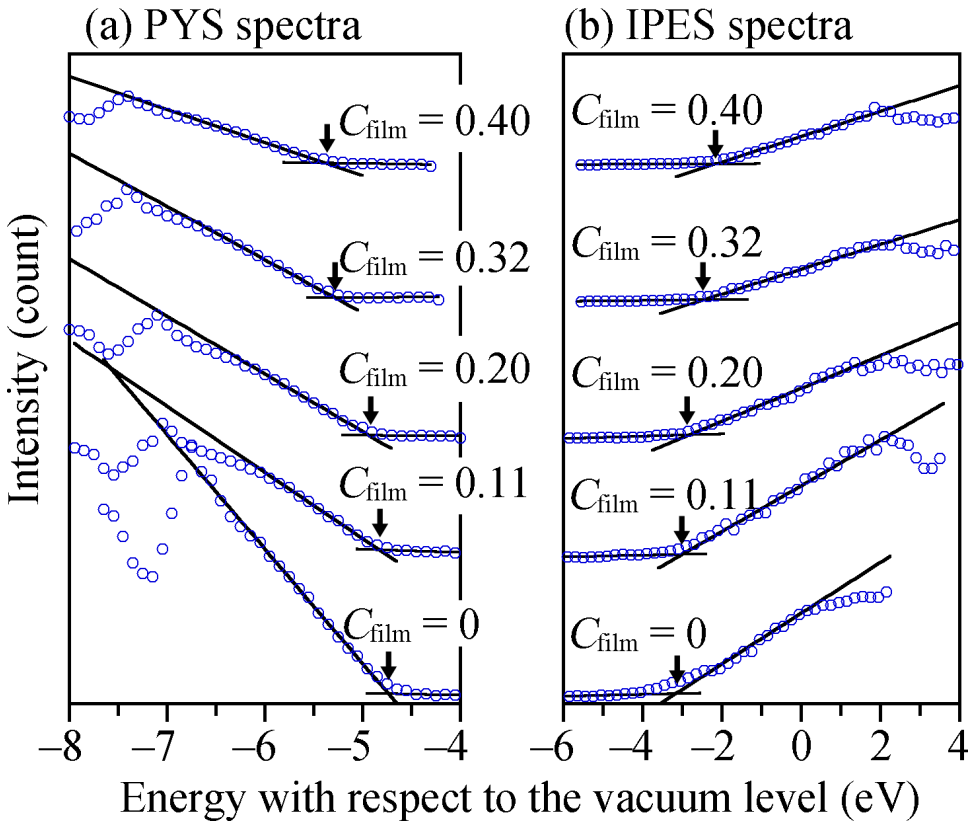

FIG. 4. (a) PYS spectra of the a-SiC films with various C_{film} displayed on a linear scale. The open circles and solid lines represent experimental and fitted data, respectively. The arrows in the figure indicate the intersection point with linear extrapolation to zero. (b) IPES spectra of the films, depicted in the same style as those in Figure 4(a).

the gap between exponential tail states.[22] Therefore, the simple equation CBM = (VBM + E_{opt}) underestimates the true CBM, as shown in Table I.

The E_{opt} increases monotonically with C_{film}, whereas the E_g exhibits an appreciable change at C_{film} = 0.2. The band widenings of E_g and E_{opt} are consistent with each other at C_{film} < 0.2. In contrast, the difference between E_g and E_{opt} abruptly increases at C_{film} > 0.2, as listed in Table I as $E_g - E_{opt}$. This result implies the exponential widening of the band tail at C_{film} > 0.2.

As aforementioned, our a-SiC film features many hydrogen atoms in the form of CH_n entities. Therefore, as in the case of the film with C_{film} > 0.2, the effect of topological and compositional disorder on the electronic structure should be considered to provide a detailed analysis. In the case of the film with C_{film} < 0.2, the incorporated C widened the E_g less effectively. The presence of C might lead to a broadening of the band tail as well as to partial cancellation of the increase of

TABLE I. Physical parameters of the investigated a-SiC films as functions of their C content.

		Experimental values					
C_{ink}	C_{film}	VBM [eV]	CBM [eV]	E_{opt} [eV]	E_g [eV] (CBM – VBM)	Estimated CBM [eV] (VBM + E_{opt})	$E_g - E_{opt}$ [eV]
0	0	−4.7	−3.1	1.54	1.6	−3.2	0.06
0.17	0.11	−4.8	−3.0	1.70	1.8	−3.1	0.1
0.31	0.20	−4.9	−2.9	1.80	2.0	−3.1	0.2
0.54	0.32	−5.3	−2.4	1.95	2.9	−3.4	0.95
0.72	0.40	−5.4	−2.3	2.02	3.1	−3.4	1.08

the E_g.[23] This behavior is well investigated on the basis of the a-Si structure because the electronic structure in a-Si holds for a-SiC with low C_{film}.[24]

In summary, we investigated a-SiC films deposited by LVD using SiC-inks with various C contents. The films were concurrently characterized by PYS and IPES, leading to precise CBM and VBM values in addition to the actual E_g. The real CBM was larger than the CBM value estimated by the simple equation CBM = VBM + E_{opt} because of the elimination of tail effects. We clarified that the tail effects were dramatically enlarged in films with higher C contents. Specifically, exponential widening of the band tail inhibited the shift of E_{opt} in the films with $C_{film} > 0.2$. Thus, the CBM estimated by the equation CBM = VBM + E_{opt} gradually deviates from the real CBM values at higher C_{film} values. These features might be related to the unusual microstructural disorder of the films. Nevertheless, the films had reasonable CBM/VBM values and exhibited good electrical properties.[13] The states were controlled by changing the composition ratio of the Si and C sources in the SiC-ink, which leads to the possibility of these films finding applications in nonvacuum-processed SiC electronics.

ACKNOWLEDGEMENTS

This work was partially funded by the Shibuya Foundation and Grants-in-Aid for Scientific Research, Japan.

[1] H. Matsunami, "Amorphous and crystalline silicon carbide II," in *Crystalline SiC on Si and High Temperature Operational Devices*, edited by M. M. Rahman, C. Y. W. Yang, and G. L. Harris (Springer-Verlag, Berlin Heidelberg, 1988), pp. 2–7.
[2] S. Yajima, Y. Hasegawa, K. Okamura, and T. Matsuzawa, Nature **273**, 525 (1978).
[3] K. J. Wynne and R. W. Rice, Annu. Rev. Mater. Sci. **14**, 297 (1984).
[4] W. H. Atwell, in *Silicon-based polymer science*, edited by J. M. Zeigler and F. W. G. Fearon (American Chemical Society, Washington, DC, 1990).
[5] Y. Hasegawa and K. Okamura, J. Mater. Sci. **18**, 3633 (1983).
[6] C. Laffon, A. M. Flank, P. Lagarde, M. Laridjani, R. Hagege, P. Olry, J. Cotteret, J. Dixmier, J. L. Miquel, H. Hommel, and A. P. Legrand, J. Mater. Sci. **24**, 1503 (1989).
[7] T. Masuda, A. Iwasaka, H. Takagishi, and T. Shimoda, J. Mater. Chem. C **3**, 12212 (2015).
[8] T. Masuda, A. Iwasaka, H. Takagishi, and T. Shimoda, J. Am. Ceram. Soc. DOI: 10.1111/jace.14138.
[9] F. Finocchi and G. Galli, Phys. Rev. B **50**, 7393 (1994).
[10] F. Evangelisti, P. Fiorini, C. Giovannella, F. Patella, P. Perfetti, C. Quaresima, and M. Capozi, Appl. Phys. Lett. **44**, 764 (1984).
[11] J. F. Muth, J. H. Lee, I. K. Shamagin, R. M. Kolbas, H. C. Casey, Jr., B. P. Keller, U. K. Mishra, and S. P. DenBaars, Appl. Phys. Lett. **71**, 2572 (1997).
[12] T. Masuda, Y. Matsuki, and T. Shimoda, Polymer **53**, 2973 (2012).
[13] T. Masuda, Z. Shen, H. Takagishi, K. Ohdaira, and T. Shimoda, Jpn. J. Appl. Phys. **53**, 031304 (2014).
[14] T. Masuda, H. Takagishi, Z. Shen, K. Ohdaira, and T. Shimoda, Thin Solid Films **589**, 221 (2015).
[15] Z. Shen, T. Masuda, H. Takagishi, K. Ohdaira, and T. Shimoda, Chem. Commun. **51**, 4417 (2015).
[16] Y. H. Wang, J. Lin, and C. H. A. Huan, Mater. Sci. Eng. B **95**, 43 (2002).
[17] L. M. Moreno and J. A. Verges, Philos. Mag. B **61**, 237 (1990).
[18] J. Robertson, Philos. Mag. B **66**, 615 (1992).
[19] J. Tauc, R. Grigorovici, and A. Vancu, Phys. Stat. Sol. **15**, 627 (1966).
[20] F. J. Himpsel and Th. Fauster, J. Vac. Sci. Technol.
[21] M. D. Seta, S. L. Wang, F. Fumi, and F. Evangelisti, Phy. Rev. B **47**, 7041 (1993).
[22] *Handbook of Photovoltaic Science and Engineering*, edited by A. Luque and S. Hegedus (John Wiley & Sons, Chichester, 2003), pp. 505–565.
[23] S. Knief and W. v. Niessen, J. Non-Cryst. Solids **255**, 242 (1999).
[24] T. M. Brown, C. Bittencourt, M. Sebastiani, and F. Evangelisti, Phys. Rev. B **55**, 9904 (1997).